Fringe fields: more relevant than the body?

Thomas Pugnat[1]
B. Dalena[1], L. Bonaventura[2], A. Simona[2],
Thanks: R. De Maria[3], V. K. Berglyd Olsen[3], R. Tomás[3], E. H. Maclean[3], O. Napoly[1], C. Lorin[1], S. Izquierdo Bermudez[3]

[1]CEA - DRF/Irfu/DACM

[2]MOX, Politecnico di Milano

[3]CERN

Mitigation Approaches for Storage Rings and Synchrotrons

22th June 2020

Contents

Motivation

In order to improve the design, performance and control of future hadronic circular colliders, does the longitudinal distribution of the magnetic fields non-linearities inside the magnet has an impact on the beam dynamic?

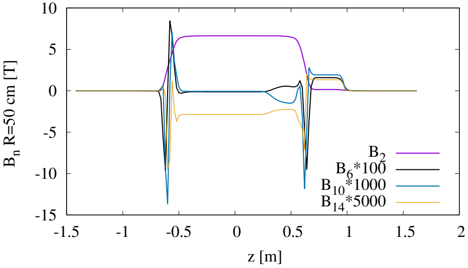

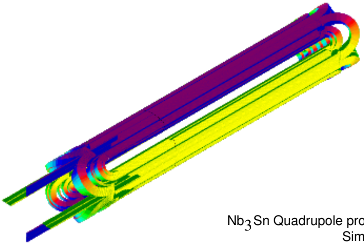

Nb_3Sn Quadrupole prototype for HL-LHC
Simulated with ROXIE
Courtesy of CERN magnet group

Goals:

- Develop a "realistic" non-linear transfer map for tracking studies.
- Use calculated or measured magnetic field map given by the magnet designers.
- Study observables sensitive to the longitudinal field description.

Contents

Definition of the Generalized Gradient

- Usually, the harmonics used for the simulation are averaged over the magnet.
- But in the harmonics profile, there is a strong variation of their strength in the extremity (geometry of the heads).

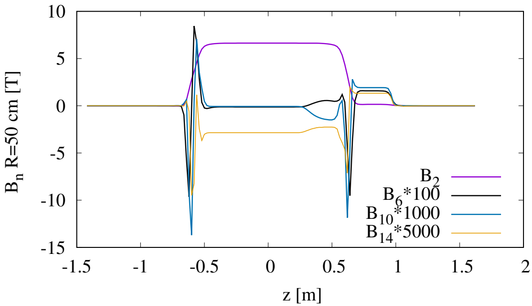

Hard Edge (S. White Ref. [1]):

$$B_y + iB_x = \sum_{n\in\mathbb{N}} (b_{n,c} + ib_{n,s})(x+iy)^n$$

$$\Downarrow$$

$$\bar{b}_{n,c} = \frac{1}{L_{Ele.}} \int_{z\in Ele.} \frac{1}{(n-1)!} \left.\frac{\partial^{n-1} B_y}{\partial x^{n-1}}\right|_{0,0,z} \mathrm{d}z$$

$$\bar{b}_{n,s} = \frac{1}{L_{Ele.}} \int_{z\in Ele.} \frac{1}{(n-1)!} \left.\frac{\partial^{n-1} B_x}{\partial x^{n-1}}\right|_{0,0,z} \mathrm{d}z$$

Using Generalized Gradient:

$$B_\rho = \sum_{n\in\mathbb{N}} B_{n,c}(R,z)\cos(n\phi) + B_{n,s}(R,z)\sin(n\phi)$$

$$\Downarrow$$

$$C_{n,u}^{[ND]}(z) = \frac{i^{ND}}{2^n n!} \frac{1}{\sqrt{2\pi}} \int_{-\infty}^{+\infty} \frac{k^{ND+n+1}}{I_n'(Rk)} \tilde{B}_{n,u}(R,k) e^{ikz}\, \mathrm{d}k \quad \text{for } u \in \{s,c\}$$

Vector potential using Generalized Gradient

$$a_x(x,y,z) = \frac{q}{p_0 c}\sum_n^\infty \sum_l^\infty \frac{(-1)^l (n-1)!}{2^{2l} l!(l+n)!} \left[\sum_{p=0}^{n/2}\sum_{q=0}^{l}\binom{n}{2p}\binom{l}{q}(-1)^p x^{n+2(l-p-q)+1} y^{2(p+q)} C_{n,s}^{[2l+1]}(z) - \sum_{p=0}^{(n-1)/2}\sum_{q=0}^{l}\binom{n}{2p+1}\binom{l}{q}(-1)^p x^{n+2(l-p-q)} y^{2(p+q)+1} C_{n,c}^{[2l+1]}(z)\right]$$

$$a_y(x,y,z) = \frac{q}{p_0 c}\sum_n^\infty \sum_l^\infty \frac{(-1)^l (n-1)!}{2^{2l} l!(l+n)!} \left[\sum_{p=0}^{n/2}\sum_{q=0}^{l}\binom{n}{2p}\binom{l}{q}(-1)^p x^{n+2(l-p-q)} y^{2(p+q)+1} C_{n,s}^{[2l+1]}(z) - \sum_{p=0}^{(n-1)/2}\sum_{q=0}^{l}\binom{n}{2p+1}\binom{l}{q}(-1)^p x^{n+2(l-p-q)-1} y^{2(p+q+1)} C_{n,c}^{[2l+1]}(z)\right]$$

$$a_z(x,y,z) = \frac{q}{p_0 c}\sum_n^\infty \sum_l^\infty \frac{(-1)^{l+1} (n-1)!(2l+n)}{2^{2l} l!(l+n)!} \left[\sum_{p=0}^{n/2}\sum_{q=0}^{l}\binom{n}{2p}\binom{l}{q}(-1)^p x^{n+2(l-p-q)} y^{2(p+q)+1} C_{n,s}^{[2l]}(z) - \sum_{p=0}^{(n-1)/2}\sum_{q=0}^{l}\binom{n}{2p+1}\binom{l}{q}(-1)^p x^{n+2(l-p-q)-1} y^{2(p+q)} C_{n,c}^{[2l]}(z)\right]$$

Building the New Transfert Map with Lie Algebra

8 D equivalent Hamiltonian for quadrupole (Y. K. Wu 2003 Ref. [2]):

$$H\left[x,p_x,y,p_y,s,\delta;z\right] = -\sqrt{(1+\delta)^2-(p_x-a_x)^2-(p_y-a_y)^2}-a_z$$

$$\Downarrow$$

$$K\left[x,p_x,y,p_y,s,\delta,z,p_z;\sigma\right] = p_z-\delta-a_z+\frac{(p_x-a_x)^2}{2(1+\delta)}+\frac{(p_y-a_y)^2}{2(1+\delta)}$$

Using the Lie Algebra formalism:

$$M(\Delta\sigma) = \exp(-L:K:)$$

But terms of the type $(p_{x,y}-a_{x,y})^2$ are not exactly solvable!
So another transformation is needed.

$$\begin{aligned}
M(\Delta\sigma) &= \exp\left(\frac{-\Delta\sigma}{2}:K1:\right)\exp\left(-\frac{\Delta\sigma}{2}:K2:\right) \\
&\quad \exp\left(:K3':\right)\exp\left(-\frac{\Delta\sigma}{2}:K3:\right)\exp\left(:-K3':\right) \\
&\quad \exp\left(:K4':\right)\exp\left(-\Delta\sigma:K4:\right)\exp\left(:-K4':\right) \\
&\quad \exp\left(:K3':\right)\exp\left(-\frac{\Delta\sigma}{2}:K3\right)\exp\left(:-K3':\right) \\
&\quad \exp\left((-\frac{\Delta\sigma}{2}:K2:\right)\exp\left(-\frac{\Delta\sigma}{2}:K1:\right)+O(\Delta\sigma^3) \\
&= M2+O(\Delta\sigma^3)
\end{aligned}$$

with: $K1 = p_z-\delta$ $\quad K3=\frac{p_x^2}{2(1+\delta)}$ $\quad K3' = \int a_x\,\mathrm{d}x$

$K2 = a_z$ $\quad K4 = \frac{p_y^2}{2(1+\delta)}$ $\quad K4' = \int a_y\,\mathrm{d}y$

The New Lie Transfert Map

$$\begin{pmatrix} p_x \\ p_y \end{pmatrix}_{i+1/7} = \begin{pmatrix} p_x \\ p_y \end{pmatrix}_i + \frac{dz}{2}\begin{pmatrix} \frac{\partial a_z(x_i,y_i,i)}{\partial x} \\ \frac{\partial a_z(x_i,y_i,i)}{\partial y} \end{pmatrix} - \begin{pmatrix} a_x(x_i,y_i,i) \\ \int \frac{\partial a_x(x_i,y_i,i)}{\partial y}\,\mathrm{d}x \end{pmatrix}$$

$$x_{i+2/7} = x_{i+1/7} + \frac{dz}{2}\frac{p_{x,i+1/7}}{1+\delta}$$

$$\begin{pmatrix} p_x \\ p_y \end{pmatrix}_{i+3/7} = \begin{pmatrix} p_x \\ p_y \end{pmatrix}_{i+2/7} + \begin{pmatrix} a_x(x_{i+2/7},y_{i+2/7},i) \\ \int \frac{\partial a_x(x_{i+2/7},y_{i+2/7},i)}{\partial y}\,\mathrm{d}x \end{pmatrix} - \begin{pmatrix} \int \frac{\partial a_y(x_{i+2/7},y_{i+2/7},i)}{\partial x}\,\mathrm{d}y \\ a_y(x_{i+2/7},y_{i+2/7},i) \end{pmatrix}$$

$$y_{i+4/7} = y_{i+3/7} + dz\frac{p_{y,i+3/7}}{1+\delta}$$

$$\begin{pmatrix} p_x \\ p_y \end{pmatrix}_{i+5/7} = \begin{pmatrix} p_x \\ p_y \end{pmatrix}_{i+4/7} + \begin{pmatrix} \int \frac{\partial a_y(x_{i+4/7},y_{i+4/7},i)}{\partial y}\,\mathrm{d}x \\ a_y(x_{i+4/7},y_{i+4/7},i) \end{pmatrix} - \begin{pmatrix} a_x(x_{i+4/7},y_{i+4/7},i) \\ \int \frac{\partial a_x(x_{i+4/7},y_{i+4/7},i)}{\partial y}\,\mathrm{d}x \end{pmatrix}$$

$$x_{i+6/7} = x_{i+5/7} + \frac{dz}{2}\frac{p_{x,i+5/7}}{1+\delta}$$

$$\begin{pmatrix} p_x \\ p_y \end{pmatrix}_{i+1} = \begin{pmatrix} p_x \\ p_y \end{pmatrix}_{i+6/7} + \begin{pmatrix} a_x(x_{i+6/7},y_{i+6/7},i) \\ \int \frac{\partial a_x(x_{i+6/7},y_{i+6/7},i)}{\partial y}\,\mathrm{d}x \end{pmatrix} + \frac{dz}{2}\begin{pmatrix} \frac{\partial a_z(x_{i+6/7},y_{i+6/7},i)}{\partial x} \\ \frac{\partial a_z(x_{i+6/7},y_{i+6/7},i)}{\partial y} \end{pmatrix}$$

Analytical Direct and Cross Amplitude Detuning

For averaged magnetic harmonics:

$$\begin{aligned}
\Delta Q_x &= \frac{q}{2\pi p_0 c}\sum_i \Bigg[\frac{3}{8}\left(\beta_x^2\bar{b}_4\right)_i (2J_x) \\
&- \frac{3}{4}\left(\beta_x\beta_y\bar{b}_4\right)_i (2J_y) \\
&+ \frac{5}{16}\left(\beta_x^3\bar{b}_6\right)_i (2J_x)^2 \\
&+ \frac{15}{16}\left(\beta_x\beta_y^2\bar{b}_6\right)_i (2J_y)^2 \\
&- \frac{15}{8}\left(\beta_x^2\beta_y\bar{b}_6\right)_i (2J_x 2J_y) \Bigg]
\end{aligned}$$

$$\begin{aligned}
\Delta Q_y &= \frac{q}{2\pi p_0 c}\sum_i \Bigg[\frac{3}{8}\left(\beta_y^2\bar{b}_4\right)_i (2J_y) \\
&- \frac{3}{4}\left(\beta_x\beta_y\bar{b}_4\right)_i (2J_x) \\
&- \frac{5}{16}\left(\beta_y^3\bar{b}_6\right)_i (2J_y)^2 \\
&- \frac{15}{16}\left(\beta_x^2\beta_x\bar{b}_6\right)_i (2J_x)^2 \\
&+ \frac{15}{8}\left(\beta_x\beta_y^2\bar{b}_6\right)_i (2J_x 2J_y) \Bigg]
\end{aligned}$$

For Generalized Gradients:

$$\begin{aligned}
\Delta Q_x &= \frac{q}{2\pi p_0 c}\sum_i \Bigg[\frac{3}{8}\left(4\beta_x^2 C_{4,s}^{[0]} + 2\beta_x\alpha_x C_{2,s}^{[1]} - \frac{2}{3}\beta_x^2 C_{2,s}^{[2]}\right)_i (2J_x) \\
&- \frac{3}{4}\left(4\beta_x\beta_y C_{4,s}^{[0]} - \frac{1}{3}(\beta_x\alpha_y - \beta_y\alpha_x) C_{2,s}^{[1]}\right)_i (2J_y) \\
&+ \frac{5}{16}\left(6\beta_x^3 C_{6,s}^{[0]} + \frac{3}{2}\beta_x^2\alpha_x C_{4,s}^{[1]} - \frac{9}{20}\beta_x^3 C_{4,s}^{[2]}\right)_i (2J_x)^2 \\
&+ \frac{15}{16}\left(6\beta_x\beta_y^2 C_{6,ts}^{[0]} + \frac{1}{5}\beta_y\left(\frac{\beta_y\alpha_x}{2} - 3\beta_x\alpha_y\right) C_{4,s}^{[1]} + \frac{3}{20}\beta_x\beta_y^2 C_{4,s}^{[2]}\right)_i (2J_y)^2 \\
&- \frac{15}{8}\left(6\beta_x^2\beta_y C_{6,s}^{[0]} - \frac{1}{5}\beta_x\left(\frac{\beta_x\alpha_y}{2} - 3\beta_y\alpha_x\right) C_{4,s}^{[1]} - \frac{3}{20}\beta_x^2\beta_y C_{4,s}^{[2]}\right)_i (2J_x 2J_y) \Bigg]
\end{aligned}$$

$$\begin{aligned}
\Delta Q_y &= \frac{q}{2\pi p_0 c}\sum_i \Bigg[\frac{3}{8}\left(4\beta_y^2 C_{4,s}^{[0]} - 2\beta_y\alpha_y C_{2,s}^{[1]} + \frac{2}{3}\beta_y^2 C_{2,s}^{[2]}\right)_i (2J_y) \\
&- \frac{3}{4}\left(4\beta_x\beta_y C_{4,s}^{[0]} - \frac{1}{3}(\beta_x\alpha_y - \beta_y\alpha_x) C_{2,s}^{[1]}\right)_i (2J_x) \\
&- \frac{5}{16}\left(6\beta_y^3 C_{6,s}^{[0]} - \frac{3}{2}\beta_y^2\alpha_y C_{4,s}^{[1]} + \frac{9}{20}\beta_y^3 C_{4,s}^{[2]}\right)_i (2J_y)^2 \\
&- \frac{15}{16}\left(6\beta_x^2\beta_y C_{6,s}^{[0]} - \frac{1}{5}\beta_x\left(\frac{\beta_x\alpha_y}{2} - 3\beta_y\alpha_x\right) C_{4,s}^{[1]} - \frac{3}{20}\beta_x^2\beta_y C_{4,s}^{[2]}\right)_i (2J_x)^2 \\
&+ \frac{15}{8}\left(6\beta_x\beta_y^2 C_{6,s}^{[0]} + \frac{1}{5}\beta_y\left(\frac{\beta_y\alpha_x}{2} - 3\beta_x\alpha_y\right) C_{4,s}^{[1]} + \frac{3}{20}\beta_x\beta_y^2 C_{4,s}^{[2]}\right)_i (2J_x 2J_y) \Bigg]
\end{aligned}$$

Contents

HL-LHC collision Optics

Why this optics?

- High luminosity Interaction Region (IR) in circular collider require very low β^* (15 cm).
  ⇒ *The beam is sensible to the non-linearities in the Final Focus magnet due to the high β-function.*
- The CERN use superconductor magnet in order to have high gradient and large aperture for HL-LHC Inner Triplet.
  ⇒ *Long magnet with strong non-linearities in the extremity.*
- The non-linear correctors in purple correct locally the non-linearities (IR by IR).

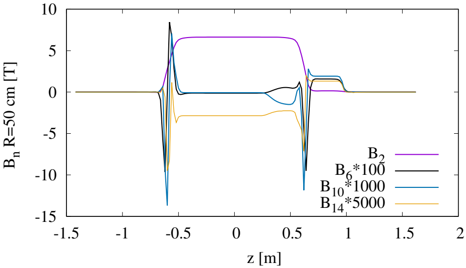

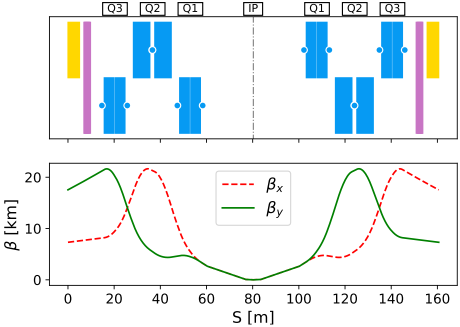

Models compared

Models compared:

1. **HE (Hard Edge):** 16 Drift and Kick of equal multipolar integrated strength.
2. **HE+Heads:** Similar to HE but with a part of the total integrated strength in additional Kick in the extremity (Ref. [3]).
3. **Lie2:** Nonlinear transfer map from Lie algebra (Ref. [4, 5, 6]). The extremities are modeled by computing the vector potential with $dz = 2\,\mathrm{cm}$.
   - **ND0:** Only pure harmonics in the Quadrupole.
   - **ND6:** with up to the 6^{th} derivative of the gradient.

The Lie2 model was developed at the CEA and is **implemented in SixTrack** (Ref. [7, 8]).

Definition of the Heads:

$$\{z \in \mathbb{R} : A_x(x,y,z) \neq 0 \text{ or } A_y(x,y,z) \neq 0,\ \forall x,y \in \mathbb{R}\}$$

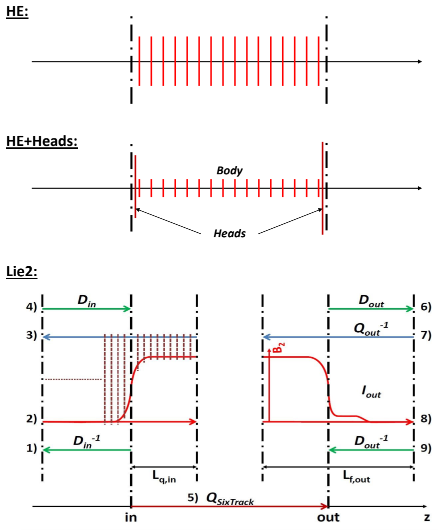

Direct Amplitude Detuning

- 1^{st} and 2^{nd} order detuning well reproduced by analytic computation.
- The impact of the harmonics longitudinal distribution (only b_6 here) is clearly measurable.
- HE+heads is a good approximation of Lie2 map, but do not account for effects due to gradients derivatives.

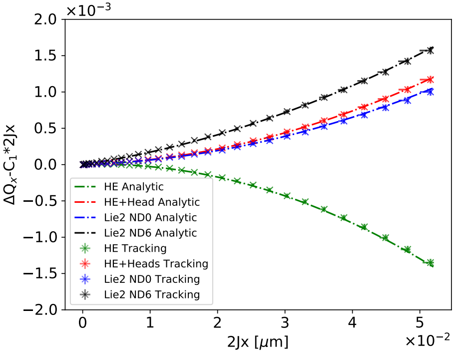

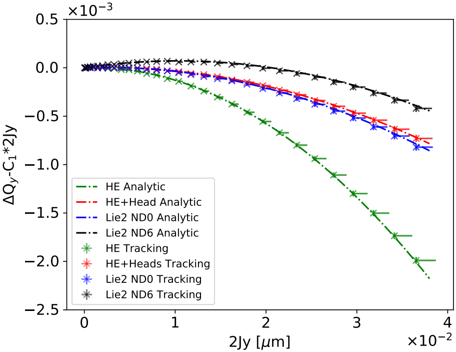

Correctors strength (Octupole corrector)

- First and second derivative of the main quadrupole field provide a systematic shift in the integrated octupole corrector strength (K3L).
- The shift is $\sim 4\%$ (K3L) with respect to correctors specification (IPAC13 WEPEA048 Ref. [9]).

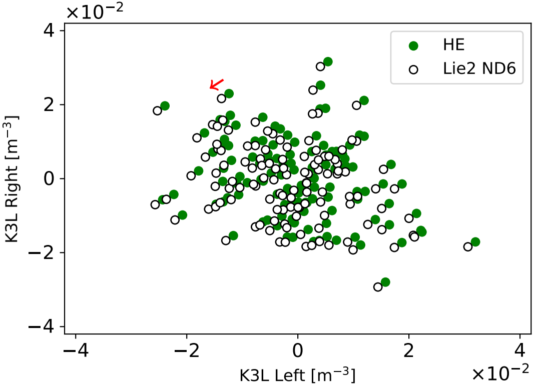

Correction procedure:

$$\begin{pmatrix} K_{(n-1),Left}L \\ K_{(n-1),Right}L \end{pmatrix} = \begin{pmatrix} \beta^{n/2}_{x,Left} & \beta^{n/2}_{x,Right} \\ \beta^{n/2}_{y,Left} & \beta^{n/2}_{y,Right} \end{pmatrix}^{-1} \sum_{s \in IP} b_{n,s} K_{r,s} L_s \begin{pmatrix} \beta^{n/2}_{x,s} \\ \beta^{n/2}_{y,s} \end{pmatrix}$$

Correctors strength (Dodecapole corrector)

- The shift is $\sim 13\%$ (K5L) with respect to correctors specification (IPAC13 WEPEA048 Ref. [9]).
- HE+heads is a good approximation of the more accurate Lie2 calculation (...gradient derivatives more than 2nd have negligible impact...).

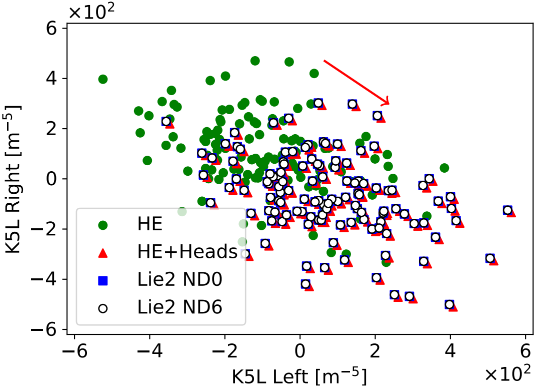

Correction procedure:

$$\begin{pmatrix} K_{(n-1),Left}L \\ K_{(n-1),Right}L \end{pmatrix} = \begin{pmatrix} \beta^{n/2}_{x,Left} & \beta^{n/2}_{x,Right} \\ \beta^{n/2}_{y,Left} & \beta^{n/2}_{y,Right} \end{pmatrix}^{-1} \sum_{s\in IP} b_{n,s}K_{r,s}L_s \begin{pmatrix} \beta^{n/2}_{x,s} \\ \beta^{n/2}_{y,s} \end{pmatrix}$$

Dynamic aperture after 10^4 revolutions

- On Axis, the DA is relatively the same for all the model while off axis, the discrepancy can be up to 2σ.
- The improvement in DA due to the b_6 correction is Model dependent.
- Statistically, the difference between the model is up to 2σ ($> 0.5\sigma$ at 10^5 turns M. Hayes 2003 Ref. [10]).
- Statistically, the correction seems more effective for the more precise model (Lie2).

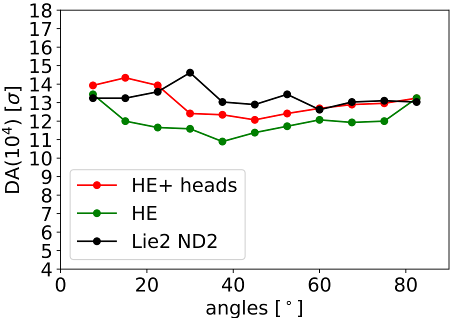

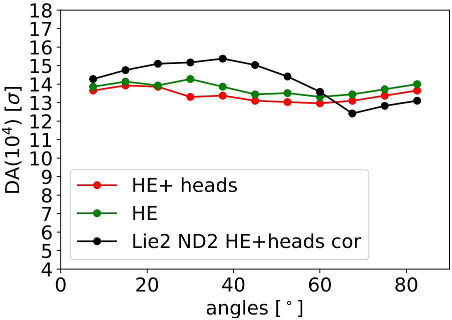

Dynamic aperture after 10^4 revolutions

- On Axis, the DA is relatively the same for all the model while off axis, the discrepancy can be up to 2σ.
- The improvement in DA due to the b_6 correction is Model dependent.
- Statistically, the difference between the model is up to 2σ ($> 0.5\sigma$ at 10^5 turns M. Hayes 2003 Ref. [10]).
- Statistically, the correction seems more effective for the more precise model (Lie2).

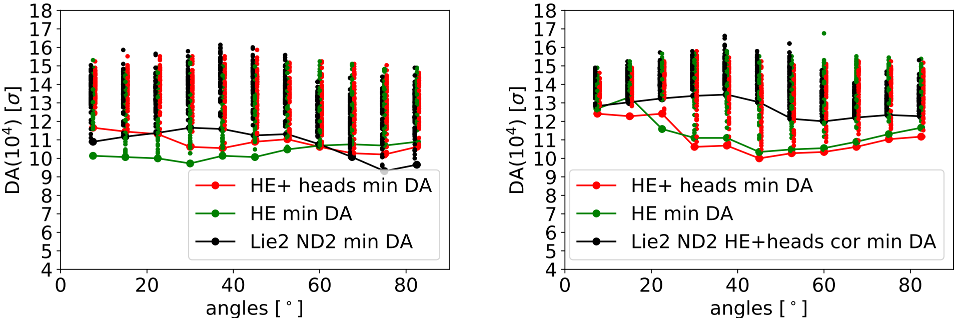

Dynamic aperture vs number of revolutions

$$DA(N) = \frac{2}{\pi} \int_0^{\pi/2} r_s(\theta;N)\,\mathrm{d}\theta$$

- The impact of the model is more significant in the first 1000 turns.
- The improvement in DA due to the b_6 correction is Model dependent.
- Statistically, for the Lie2 Model, the spread is smaller with the b_6 correction.

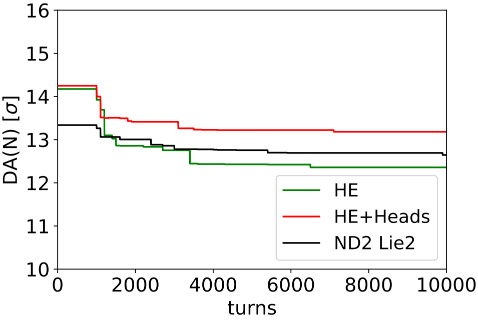

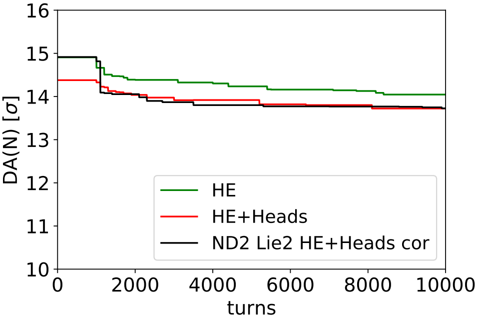

Dynamic aperture vs number of revolutions

$$DA(N) = \frac{2}{\pi}\int_0^{\pi/2} r_s(\theta;N)\,\mathrm{d}\theta$$

- The impact of the model is more significant in the first 1000 turns.
- The improvement in DA due to the b_6 correction is Model dependent.
- Statistically, for the Lie2 Model, the spread is smaller with the b_6 correction.

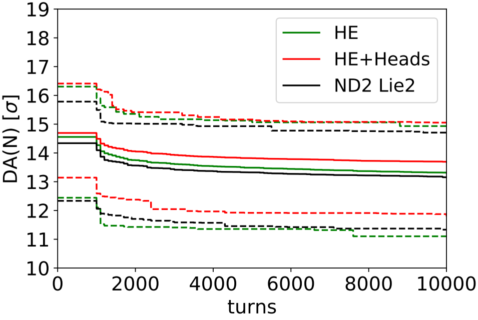

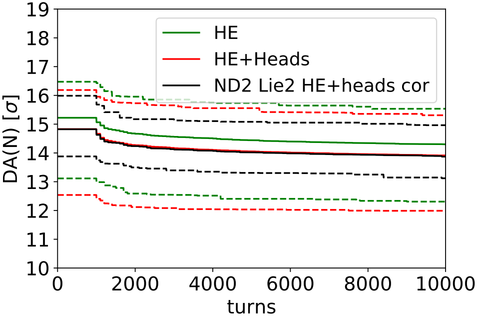

Contents

A strong b_4 and b_6 in the IT quadrupole extremity.

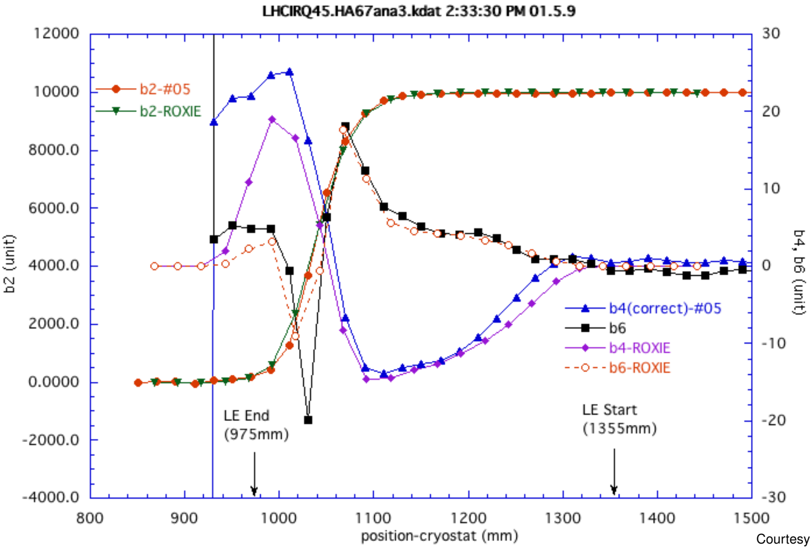

Courtesy of T. Nakamoto (KEK).

Correctors strength

- The longitudinal distribution of b_4 in one family of the LHC Inner Triplet (Q1 and Q3) produces a small shift toward beam-based values for IR5, the inverse for IR1.
- Direct 2^{nd} order detuning not observed up to now in LHC.
- The longitudinal distribution of b_6 in one family of the LHC Inner Triplet (Q1 and Q3) reduces significantly the required correctors strength.

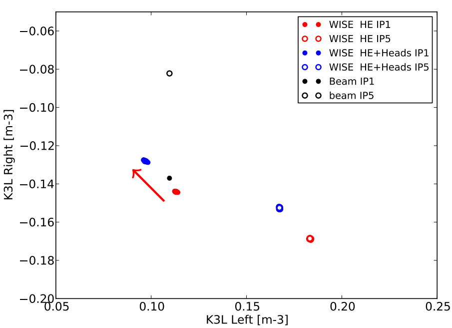

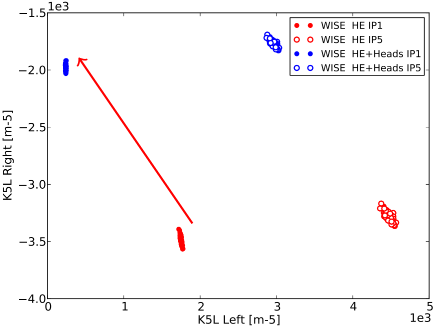

Contents

Sensibility of Amplitude Beta-Beating *(Preliminary results)*

- Resonance Driving Terms (RDTs) acting on the Spectral Ray H(-1,0) and/or V(0,-1) cause a variation of the measured β-function.

  We call it Direct and Cross Amplitude Beta-Beating (ABB).

  - *Octupolar RDTs:*

    $f_{3100}, f_{2011}, f_{1120}$ and f_{0031}
  - *Dodecapolar RDTs:*

    $f_{4200}, f_{3111}, f_{2022}, f_{2220}, f_{1131}$ and f_{0042}

- In HL-LHC simulation, an ABB of $\sim 1-2\%$ appears at an amplitude of $0.02\,\mu$m.

- The Direct and Cross Amplitude Beta-Beating seems also sensible to the harmonics longitudinal distribution.

Simulation for HL-LHC with HE (b4 errors only):

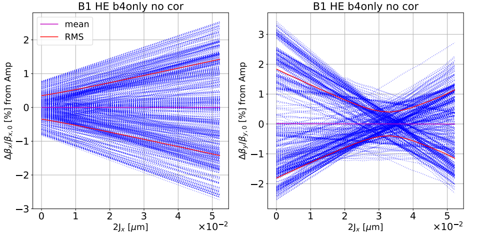

Simulation for HL-LHC with HE (b6 errors only):

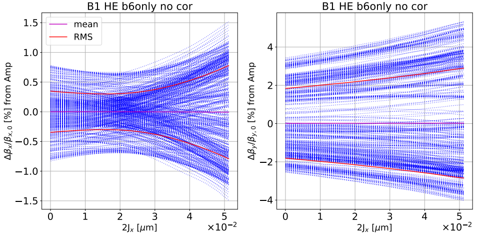

Sensibility of Amplitude Beta-Beating *(Preliminary results)*

- Resonance Driving Terms (RDTs) acting on the Spectral Ray H(-1,0) and/or V(0,-1) cause a variation of the measured β-function.

  We call it Direct and Cross Amplitude Beta-Beating (ABB).

  - *Octupolar RDTs:*

    $f_{3100}, f_{2011}, f_{1120}$ and f_{0031}
  - *Dodecapolar RDTs:*

    $f_{4200}, f_{3111}, f_{2022}, f_{2220}, f_{1131}$ and f_{0042}

- In HL-LHC simulation, an ABB of $\sim 1-2\%$ appears at an amplitude of 0.02 μm.

- The Direct and Cross Amplitude Beta-Beating seems also sensible to the harmonics longitudinal distribution.

Simulation for HL-LHC with HE (b4 errors only):

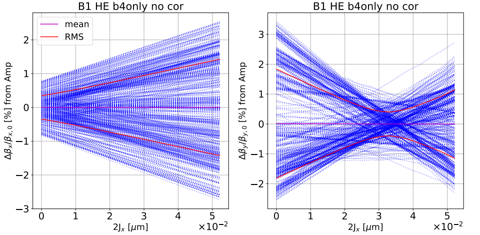

Simulation for HL-LHC with HE+Head (b6 errors only):

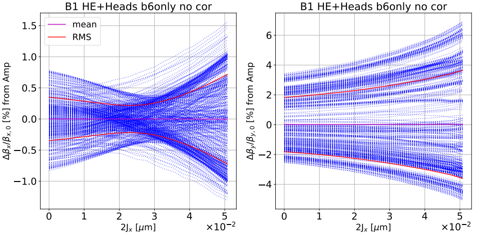

Generate a strong Amplitude Beta-Beating with octupole correctors *(Preliminary results)*

Measure on LHC (b4 not corrected):

- The variation of the ABB measured on the LHC is more compatible with noise than with actual ABB.

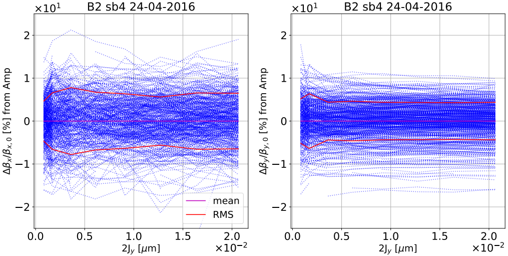

Experiment proposal on the LHC(?)

- Some configuration are analysed to generate an ABB of $\sim 10\%$ at an amplitude of 0.01 μm.
- Analytical prediction of ABB: work in progress.

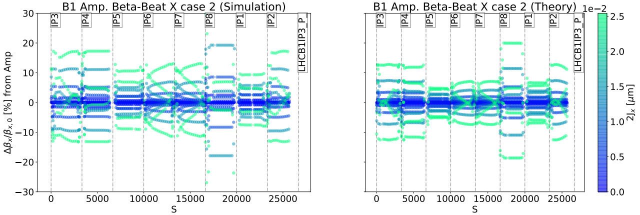

Generate a strong Amplitude Beta-Beating with octupole correctors *(Preliminary results)*

Measure on LHC (b4 not corrected):

- The variation of the ABB measured on the LHC is more compatible with noise than with actual ABB.

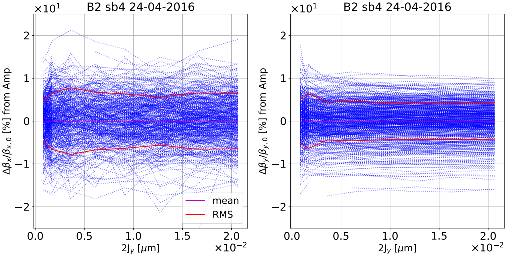

Experiment proposal on the LHC(?)

- Some configuration are analysed to generate an ABB of $\sim 10\%$ at an amplitude of 0.01 μm.
- Analytical prediction of ABB: work in progress.

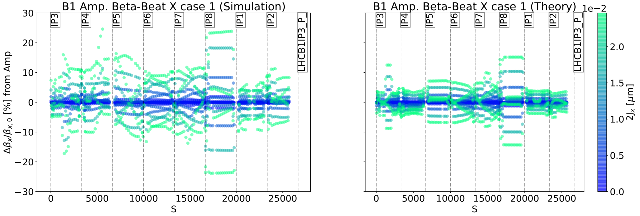

Contents

Conclusion

Analytical expressions and a new transfer map have been developed in order to take into consideration the impact of the 3D-field on beam-based observable.
(Amplitude Detuning, Correctors strength, Dynamic Aperture, Amplitude β-Beating)

For HL-LHC:

- The main field derivatives have small impact on b_4 correction ($\sim 4\%$).
- The impact of the longitudinal distribution of b_6 can be well approximated by splitting the magnet in 2 Heads + Body and it results in a shift of $\sim 13\%$ for HL-LHC optics.
- Accurate measurements of the longitudinal harmonics are important when comparing accelerators models with beam based values. In particular, there is no ROXIE model is available for the not allowed ones (b_3, b_4, b_5, . . . for quad).
- The improvement in the minimal DA is model dependent.

For LHC:

- The b_4 longitudinal distribution (in Q1 and Q3) produces a small shift with respect to WISE integrated value which increases the puzzle of octupole correction in LHC.
- The b_6 longitudinal distribution (in Q1 and Q3) has a big impact on the dodecapole correctors strength. But is hard to predict a precise value since there are no information of the b_6 longitudinal distribution inside Q2.
- The present Amplitude β-Beating due to higher order harmonics is in the percent level. The measurement is hidden in the noise. But some LHC configuration can provide an Amplitude β-Beating of $\sim 10\%$ at 0.01 μm

So YES, the harmonics longitudinal distribution has an impact on beam based quantities, but is more relevant when the actual collider configuration is known than in the design phase.

Bibliography

[1] *Direct amplitude detuning measurement with ac dipole*
S. White, E. H Maclean, and R. Tomas,
in *Phys. Rev. STAB*, vol. 16, pp. 046502, Jul. 2013.

[2] *Explicit symplectic integrator for s-dependent static magnetic field*
Y. K. Wu, E. Forest and D. S. Robin,
in *Phys. Rev. E*, vol. 68, pp. 046502, Oct. 2003.

[3] *Dynamic aperture studies for HL-LHC V1.0*,
Y. Cai *et al.*,
CERN-ACC-2018-0054.

[4] *Fringe Field Modeling for the High Luminosity LHC Large Aperture quadrupole*,
B. Dalena *et al.*,
in *Proc. IPAC'14*, Dresden, Germany, June 2014, paper TUPRO002, pp. 993-996.

[5] *Accurate and Efficient Tracking in Electromagnetic Quadrupoles*,
T. Pugnat *et al.*,
in *Proc. IPAC'18*, Vancouver, Canada, June 2014, paper THPAK004, pp. 3207-3210.

[6] *High order time integrators for the simulation of charged particle motion in magnetic quadrupoles*,
A. Simona *et al.*,
Comp. Phys. Comm., vol. 239, pp. 33-52, Feb. 2019.

[7] SixTrack,
`http://sixtrack.web.cern.ch/SixTrack`

[8] *SixTrack version 5: Status and new developments*,
R. De Maria *et al*,
in *Proc. IPAC'19*, Melbourne, Australia, May 2019, paper WEPTS043, pp. 3200-3203

[9] *Specification of a system of correctors for the Triplets and separation dipoles of the LHC upgrades*,
M. Giovannozzi, S. D. Fartoukh and R. De Maria,
in *Proc. IPAC'13*, Shanghai, China, Jun. 2013, paper WEPEA048, pp. 32612-2614

[10] *The influence of Computer Errors on Dynamic Aperture Results Using SixTrack*,
M. Hayes, E. McIntosh and F. Schmidt,
in *LHC Project Note 309*, Geneva, Switzerland, Jan. 2003